



Chemical evolution of galaxies and GRB cosmic rate

F. Matteucci^{1,2}, V. Grieco¹, and L. Vincoletto¹

¹ Department of Physics, Astronomy Division, Trieste University, Via Tiepolo 11, I-34131 Trieste, Italy

² Istituto Nazionale di Astrofisica - Osservatorio Astronomico di Trieste, Via Tiepolo 11, I-34131 Trieste, Italy e-mail: matteucc@oats.inaf.it

Abstract. The chemical evolution of galaxies of different morphological type (ellipticals, spirals and irregulars) is reviewed. In particular, the basic ingredients necessary to build chemical evolution models are summarized together with the basic equations and the recipes to compute supernova rates. Some highlights in the chemical evolution of galaxies are presented such as the evolution of abundances and abundance ratios in galaxies with different histories of star formation. A special attention is devoted to the fact that the abundances of different elements evolve in different ways according to their stellar origin: in particular, some chemical elements, such as α -elements, are produced on short timescales whereas others, such as Fe, on much longer ones. In addition, some elements have a primary origin (C,O,Fe) whereas others have a secondary origin (N), namely their production depends on the initial stellar metallicity. As a consequence of this, one should be very careful when defines the observed *metallicity* only on the basis of specific chemical elements. Finally, the computation of SN rates and in particular of SNe Ib/c, which are related to GRBs, is shown. The cosmic Type Ib/c SN rate, derived from the cosmic star formation rate, is compared to the observed cosmic GRB rate: the conclusion arises that the GRBs should be only a small fraction of the Type Ib/C SNe in all galaxies.

Key words. Galaxies : evolution Stars: supernovae

1. Introduction

The chemical evolution of galaxies studies the evolution in space and time of the abundances of the most common chemical elements in the interstellar medium (ISM). To build chemical evolution models one needs to have some basic ingredients at disposal. In particular, the basic ingredients are: i) the initial conditions (system closed or open) which include the assumption of the chemical composition of the

first gas. This can be primordial, namely without metals (defined as all the elements heavier than He), or pre-enriched by a first generation of stars (Population III stars).ii) The history of star formation which includes the star formation rate (SFR) and the initial mass function (IMF), iii) the stellar nucleosynthesis, namely the “stellar yields”, iv) possible gas flows. Once these quantities have been specified and the stellar lifetimes taken into account, the main equations of chemical evolution can be solved only numerically. Galaxies have dif-

Send offprint requests to: F.Matteucci

ferent morphologies and different stellar populations; these differences are mainly due to the different history of star formation (SFR+IMF) that every galaxy has suffered. Good models of chemical evolution of galaxies are aimed at reproducing the majority of the observational constraints of local galaxies. These constraints include the amount of gas and its chemical composition, the present time SFR, SN rates and the variation of the chemical abundances as a function of galactocentric distance (e.g. abundance gradients). We will show here the results of models of chemical evolution devised for galaxies of different morphological type (ellipticals, spirals and irregulars). Their evolution is characterized by different histories of star formation which predict a different behaviour for the evolution of either the absolute abundances or the abundance ratios of the chemical elements. Different chemical elements evolve in a different way for two reasons: first, because different elements are produced in different stars and by means different nucleosynthesis processes and second, because of different histories of star formation. Therefore, the use of the word “metallicity” should be made with caution since only oxygen, which is the most abundant element among metals, can trace the global metallicity Z . The supernovae of all types (Ia, Ib/c, II) are taken into account and their rates are computed as functions of cosmic time. Particularly important for the topic of this workshop are the SNe Ib/c which are likely to be the progenitors of long GRBs. These supernovae are believed to originate from massive stars ($M > 25M_{\odot}$) either single or in binary systems where the masses of the systems can range from ~ 15 to $45M_{\odot}$. Assumptions concerning the SN Ib/c progenitors together with a chosen cosmic star formation rate (CSFR, namely the SFR in a co-moving unitary volume of Universe) allow us to compute the cosmic Type Ib/c SN rate and to compare it with the observed cosmic GRB rate.

2. The SFRs in galaxies

Following the studies of Kennicutt (1989, 1998) we assume that the SFR varies along

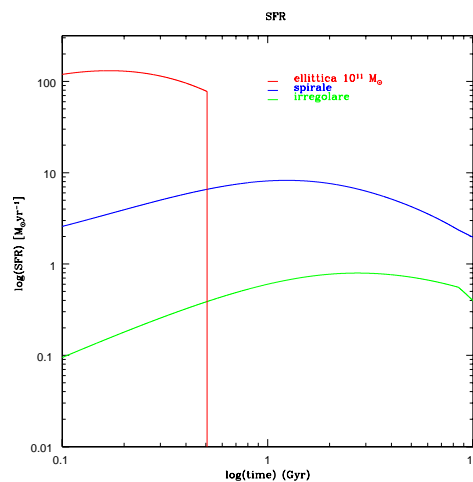


Fig. 1. The history of star formation in galaxies of different morphological type. The elliptical galaxy has an assumed baryonic mass of $10^{11} M_{\odot}$, the spiral has a baryonic mass of $5 \cdot 10^{10} M_{\odot}$ and the irregular of $10^9 M_{\odot}$.

the Hubble sequence: in particular, elliptical galaxies should have suffered an intense and rather short burst of star formation, halted by a sudden galactic wind triggered by SN explosions and/or AGN activity. Spiral and irregular galaxies should have instead suffered a continuous and milder star formation during all the galactic lifetime.

In Figure 1 we show the adopted SFRs in galaxies of different morphological type. The adopted star formation law for all these galaxies is the Kennicutt (1998) law ($SFR \propto \sigma_{gas}^k$ with $k \sim 1.5$), where only the efficiency of star formation changes for different galaxies. The efficiency of star formation is defined as the inverse of the timescale of star formation, namely the time in which all the gas in a galaxy will be consumed. For ellipticals this efficiency is assumed to be higher by an order of magnitude than the one in spirals and by two orders of magnitude than the one in irregulars (see Calura & al. 2009, for details on the models). In all the galaxy models we adopted a constant in time Salpeter (1955) IMF.

In Figure 2 we report the predicted behaviour of the global metallicity Z as a func-

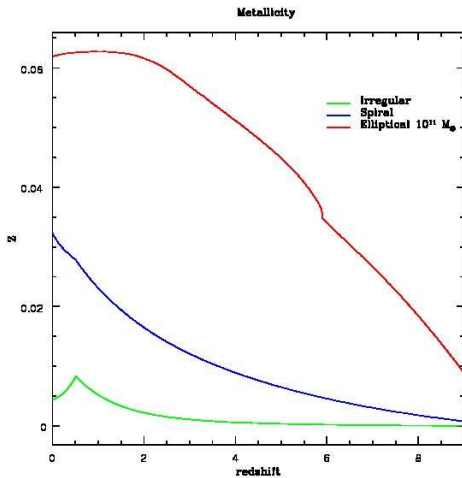


Fig. 2. Predicted metallicity evolution in galaxies of different morphological type. The galaxies are the same as in Figure 1.

tion of redshift for the three types of galaxies of Figure 1. As one can see from Figure 2, the metallicity of ellipticals is higher than the metallicity of spirals and irregulars during all the lifetime of the Universe. We recall that the solar metallicity is $Z_{\odot} \sim 0.0134$ (Asplund & al. 2009).

3. Abundance ratios in galaxies

The best studied galaxy is indeed the Milky Way, for which we have a large collection of high resolution data. In particular the abundances in the stars of the halo, thick-, thin-disk and bulge are now well measured and can be compared with the predictions from chemical models. As an example, in Figure 3 are shown abundance ratios ($[X/Fe]$) relative to the Sun for stars in the solar vicinity belonging to the halo and disk. Overimposed to the data are the predictions obtained by means the two-infall model by Chiappini et al. (1997) (where a detailed description can be found) by adopting different stellar yields. As one can see, for some elements, such as the α -elements (O, Si, S, Ca) there is a good agreement between model predictions and data, whereas for other elements such as N, Na, K and Sc, the agree-

ment is still poor. The reason for that resides indeed in the stellar yields which need still to be improved. An important fact is that different chemical elements evolve in a different way: the $[\alpha/Fe]$ ratios vs. $[Fe/H]$ show values higher than zero (corresponding to the Sun in the $[\]$ notation) in halo stars and then the ratios decrease for higher $[Fe/H]$ until the solar value is reached. This behaviour is commonly interpreted as due to the different roles played by core-collapse (II, Ib/c) SNe and thermonuclear SNe (Ia) in enriching the ISM. Type Ia SNe are assumed to originate from white dwarfs in binary systems and their rate is computed according to Matteucci & Recchi (2001). In fact, in the early phases of galactic evolution only the core-collapse SNe contribute to the chemical enrichment and they produce mainly α -elements as well as a small amount of Fe on very short timescales. When SNe Ia start exploding and restoring the bulk of Fe, on much longer timescales, then the $[\alpha/Fe]$ ratios decline. This interpretation can be applied to any abundance ratio.

3.1. Abundance ratios and different SFRs

In Figure 4 are shown the predicted $[\alpha/Fe]$ vs. $[Fe/H]$ relations when adopting different SFR histories. In particular, for a bulge like that of the Milky Way, the $[\alpha/Fe]$ ratios are predicted to be above solar for a larger range of $[Fe/H]$ than in the solar neighbourhood and in an irregular galaxy. The same behaviour applies to elliptical galaxies. The reason for that resides in the fact that during the strong starburst, characterizing the spheroid formation, the core-collapse SNe produce Fe quickly and when Type Ia SNe, which by the way are the main producers of Fe, start exploding, the ISM has already reached the solar value for $[Fe/H]$. Some data for the Galactic Bulge are shown for comparison although more recent and larger data sample for the Bulge are available and agree even better with our model (see Cescutti & Matteucci, 2011). The opposite occurs when the SFR is milder than in the solar vicinity, like in an irregular galaxy. Here, when the Type Ia SNe start restoring Fe, the Fe in the ISM

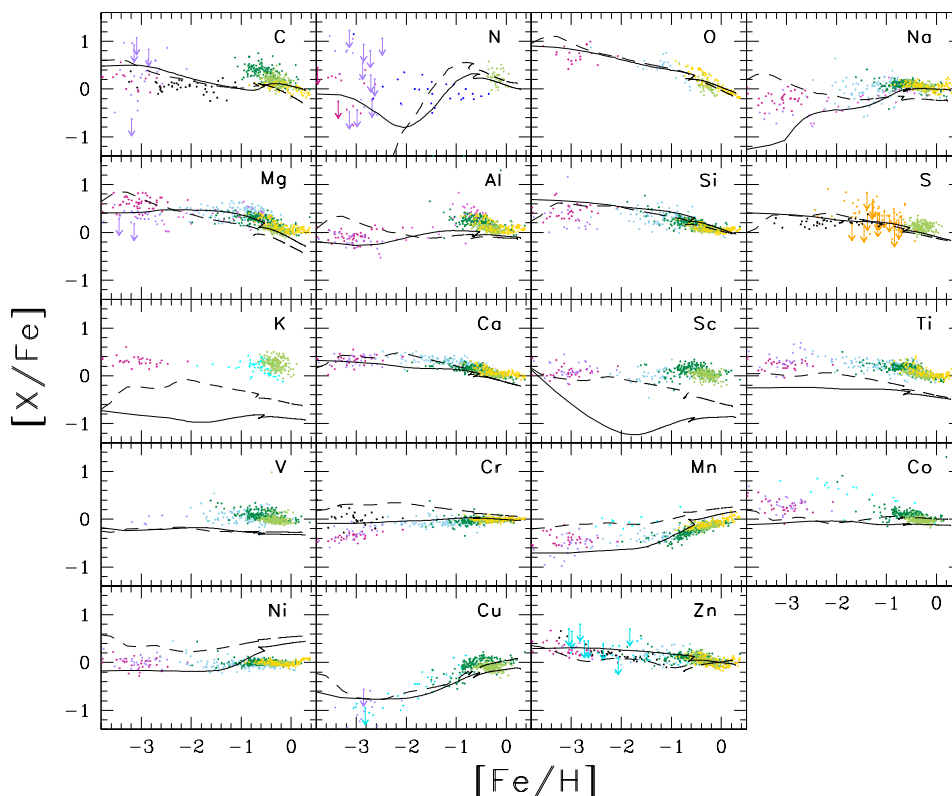


Fig. 3. $[X/Fe]$ versus $[Fe/H]$ relations for elements from C to Zn in the solar neighbourhood. The predictions are represented by the dashed and solid curves. Dashed curves are obtained by adopting the yields from Geneva group from massive stars for He, C and O, whereas the yields from massive stars for heavier elements are from Kobayashi et al. (2006). The yields from low and intermediate mass stars are from Karakas (2010). Solid curves refer to the yields of Woosley & Weaver (1995) for massive stars and to the yields of van den Hoek & Groenewegen (1996) for low and intermediate mass stars. The Figure and references to the data can be found in Romano & al. (2010).

is still quite low. The diagram of Figure 4 is interesting also because one can use it to infer the nature and the ages of unidentified high redshift objects. In fact, in Figure 4 are also reported data for Damped Lyman- α systems (DLAs) which fall on the curve for irregular galaxies, thus suggesting that DLAs can indeed be irregular galaxies.

4. Galaxies hosting GRBs

It has been suggested (Fruchter et al. 2006) that the hosts of GRBs, at least locally, are preferentially low metallicity irregular galax-

ies. We show in Figure 5 the Type Ib/c SN rates, as predicted by our models for spirals and irregulars, compared with the observed SN rates. In the same Figure it is reported the local GRB rate, and as one can see, the ratio between the GRB and Type Ib/c SN rates in irregulars is higher than in spirals. The Type Ib/c SN rates are computed by assuming that these SNe originate partly from close massive binary systems ($\sim 33\%$) and partly from single WR stars (Grieco et al. in preparation). The Type Ib/c SN rates strictly follow the SFRs of galaxies, as shown in Fig. 1.

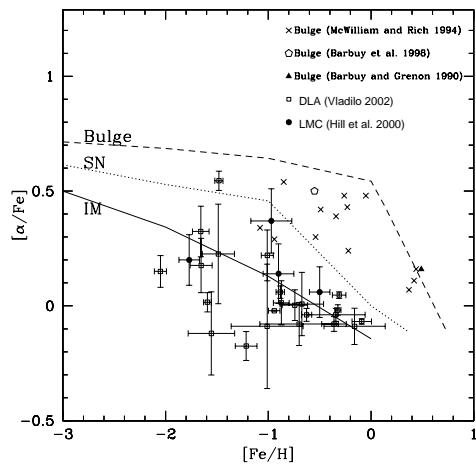


Fig. 4. Predicted $[\alpha/\text{Fe}]$ vs. $[\text{Fe}/\text{H}]$ relations in galaxies of different morphological type. Data are shown for comparison. Here, instead of an elliptical of $10^{11} M_{\odot}$ is shown a bulge of $\sim 10^{10} M_{\odot}$. Data for the Galactic Bulge as well as for the LMC and DLAs are shown for comparison.

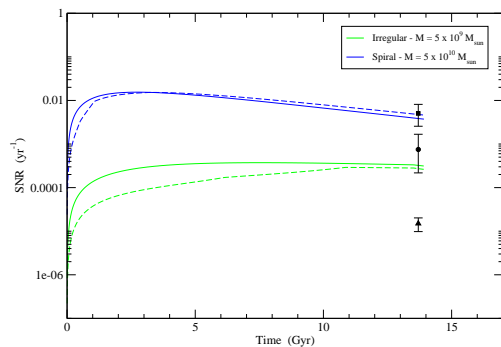


Fig. 5. The supernova Ib/c rate as a function of time for an irregular (green line) and a spiral galaxy (blue line). The continuous and dashed curves refer to a constant minimum mass of WR stars and to a mass varying with metallicity, respectively. The observed rates from Mannucci et al. (2005) are shown for comparison. In the Figure is shown also the local GRB rate.

5. The cosmic Type Ib/c SN and GRB rates

Here, we have computed also the cosmic Type Ib/c SN rate (the rate in a comoving unitary

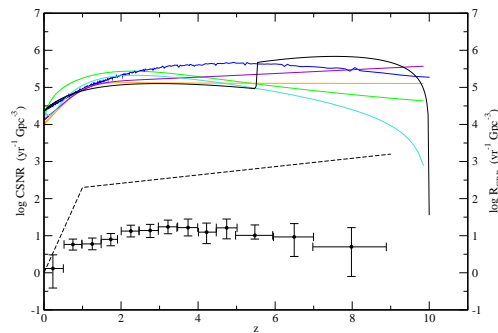


Fig. 6. Comparison between the cosmic predicted Type Ib/c SN rates computed by means of several CSFRs existing in the literature and the number of observed GRB at different redshift as provided by Wanderman & Piran (2010) from *Swift* data, black circle and Matsubayashi et al. (2005) (black dashed line). The CSNRs are computed by means of different CSFRs: in particular, the CSFR based on our models (black line), the CSFR of Menci et al. (2004) (blue line), Strolger et al. (2004) (turquoise line), Steidel et al. (1999) (orange line) and Porciani & Madau (2001) (violet line). The green line is the CSNR Ib/c based on the fit to the observed CSFR, as provided by Cole et al. (2001)

volume of the Universe) obtained by convolving the CSFR with the progenitor models for such supernovae. It is worth noting that the CSFR not necessarily follows the SFRs in galaxies since it depends also on the number density of galaxies at any given redshift and this quantity is likely to be not constant. The cosmic Type Ib/c SN rate is expressed in units of $Gpc^{-3} yr^{-1}$ and compared to the observationally derived cosmic GRB rate. In particular, in Figure 6 we show different cosmic Type Ib/c SN rates obtained by considering different CSFRs. As one can easily see from Fig. 6, the ratio between the GRBs and the SNIb/c is quite low ($\sim 10^{-3} - 10^{-4}$). However, these values should be taken with caution since the sample of Swift GRBs observed by Wanderman & Piran (2010) might not be complete and the GRB rate of Matsubayashi et al. (2005) is semi-empirical. More data on the cosmic GRB rate are necessary before drawing firm conclusions on this point.

References

- Asplund, M., Grevesse, N., Sauval, A.J. & Scott, P., 2009, *ARA&A*, 47, 481
- Barbuy, B. & Grenon, M., in *Bulges of Galaxies*, eds. B.J. Jarvis & D.M. Terndrup, ESO/CTO Workshop, p. 83
- Calura, F., Pipino, A., Chiappini, C., Matteucci, F. & Maiolino, R., 2009, *A&A*, 504, 373
- Cescutti, G. & Matteucci, F., 2011, *A&A*, 525, 126
- Chiappini, C., Matteucci, F. & Gratton, R., 1997, *ApJ*, 477, 765
- Cole, S., Norberg, P. & Baugh, C.M., 2001, *MNRAS*, 326, 255
- Hill, V., François, P., Spite, M., Primas, F. & Spite, F., 2000, *A&A*, 364, L19
- Karakas, A.I., 2010, *MNRAS*, 403, 1413
- Kennicutt, R.C. Jr., 1989, *ApJ*, 344, 685
- Kennicutt, R.C. Jr., 1998, *ApJ*, 498, 541
- Mannucci, F., Della Valle, M., Panagia, N. et al., 2005, *A&A*, 433, 807
- Matteucci, F. & Recchi, S., 2001, *ApJ*, 558, 351
- Matsubayashi, T., et al. 2005, *PThPh*, 114, 983
- Mc William, A. & Rich, R.M., 1994, *ApJS*, 91, 749
- Menci, N., et al. 2004, *ApJ*, 604, 12
- Fruchter, A.S., et al., 2006, *Nature*, 441, 463
- Kobayashi, C., et al. 2006, *ApJ*, 653, 1145
- Romano, D., Karakas, A.I., Tosi, M. & Matteucci, F., 2010, *A&A*, 522, 32
- Porciani, C. & Madau, P., 2004, *ApJ*, 548, 522
- Salpeter, E.E., 1955, *ApJ*, 121, 161
- Steidel, C.C., et al. 1999, *ApJ*, 519, 1
- Strolger, L.-G. & al., 2004, *ApJ*, 613, 200
- van den Hoek, L.B. & Groenewegen, M.A.T., 1997, *A&AS*, 123, 305
- Vladilo, G., 2002, *A&A*, 391, 407
- Wanderman, D. & Piran, T., 2009, *MNRAS*, 406, 1944
- Woosley, S.E. & Weaver, T.A., 1995, *ApJS*, 101, 181